



Large-deviation quantification of boundary conditions on the Brazil nut effectGustavo H. B. Martins *Programa de Pós Graduação em Modelagem Matemática e Computacional, Centro Federal de Educação Tecnológica de Minas Gerais–CEFET-MG. Av. Amazonas 7675, 30510-000, Belo Horizonte, Minas Gerais, Brazil*Welles A. M. Morgado *Departamento de Física, Pontifícia Universidade Católica, 22452-970, Rio de Janeiro, Rio de Janeiro, Brazil, and National Institute of Science and Technology for Complex Systems, Brazil*Sílvio M. Duarte Queirós *Centro Brasileiro de Pesquisas Físicas, R. Dr. Xavier Sigaud 150, 22290-180, Rio de Janeiro, Rio de Janeiro, Brazil; i3N, Universidade de Aveiro, Campus de Santiago, 3810-193 Aveiro, Portugal; and National Institute of Science and Technology for Complex Systems, Brazil*Allbens P. F. Atman **Departamento de Física, Centro Federal de Educação Tecnológica de Minas Gerais – CEFET-MG. Av. Amazonas 7675, 30510-000, Belo Horizonte, Minas Gerais, Brazil, and Institute of Science and Technology for Complex Systems, Brazil*

(Received 18 February 2020; revised 1 April 2021; accepted 28 April 2021; published 4 June 2021)

We present a discrete element method study of the uprising of an intruder immersed in a granular media under vibration, also known as the Brazil Nut Effect. Besides confirming granular ratcheting and convection as leading mechanisms to this odd behavior, we evince the role of the resonance on the rising of the intruder by using periodic boundary conditions (pbc) in the horizontal direction to avoid wall-induced convection. As a result, we obtain a resonance-qualitylike curve of the intruder ascent rate as a function of the external frequency, which is verified for different values of the inverse normalized gravity Γ , as well as the system size. In addition, we introduce a large deviation function analysis which displays a remarkable difference for systems with walls or pbc.

DOI: [10.1103/PhysRevE.103.062901](https://doi.org/10.1103/PhysRevE.103.062901)**I. INTRODUCTION**

Granular materials exhibit a number of startling phenomena that play a central role in various human activities and yet defy a comprehensive theoretical description [1–9]. Among them, the Brazil Nut Effect (BNE) [10,11] is a paradigmatic example of segregation, when an intruder (a grain of different size or density [12–14] compared to its surroundings) rises to the surface of a box or container under external vibration [15–19]. Since the original theoretical description made by Rosatto *et al.* [15], several real and computational experiments as well as further theoretical approaches pointed out two main mechanisms to explain this perplexing behavior: wall friction-induced convection [20] and granular ratcheting phenomena [16]. Subsequent studies to Ref. [15] showed such systems experience different regimes, depending on the characteristic acceleration of the system $a = \omega^2 A$, normalized by the acceleration of gravity g , defining its factor $\Gamma \equiv a/g$ [11] (ω is the angular frequency and A is the amplitude of the oscillations). For $\Gamma > 1$, when the system is pushed up, the confining medium behaves liquidlike and the intruder displaces particles from the medium mainly due to its greater

inertia, but when it is pulled down, the medium responds as solidlike and the intruder becomes stuck, a mechanism known as “granular ratchet” which is responsible for the “reverse buoyancy” observed in these systems. Similarly, for dense dry granular media, the granular gaslike approximation does not work [5]. Despite various efforts to identify the role of boundary conditions (walls), friction coefficients, interstitial fluid [21], and intruder geometry, among others, a comprehensive theory to describe the BNE is still missing [22]. It is noteworthy that, in addition to the condition $\Gamma > 1$, frequency in itself is also an important control parameter for the BNE phenomenon. By changing the geometry, coefficients of friction, and wall properties, there is a change in the frequency range in which the BNE is observed [16].

In this paper, we went a step further to understand this intriguing physical phenomenon by presenting a rationale to predict that the system should resonate to some characteristic frequency of the external vibrations since the grains are modeled as masses connected by slightly subcritical dissipative springs and subjected to an external sinusoidal force. Thus, by means of an innovative analysis, we calculate the large deviation function (ldf) which turns out to be an important metric to characterize different behaviors onto this granular problem. We conclude interpreting the ldf results to evidence the role of the boundary on the system dynamics and that, in

*atman@cefetmg.br

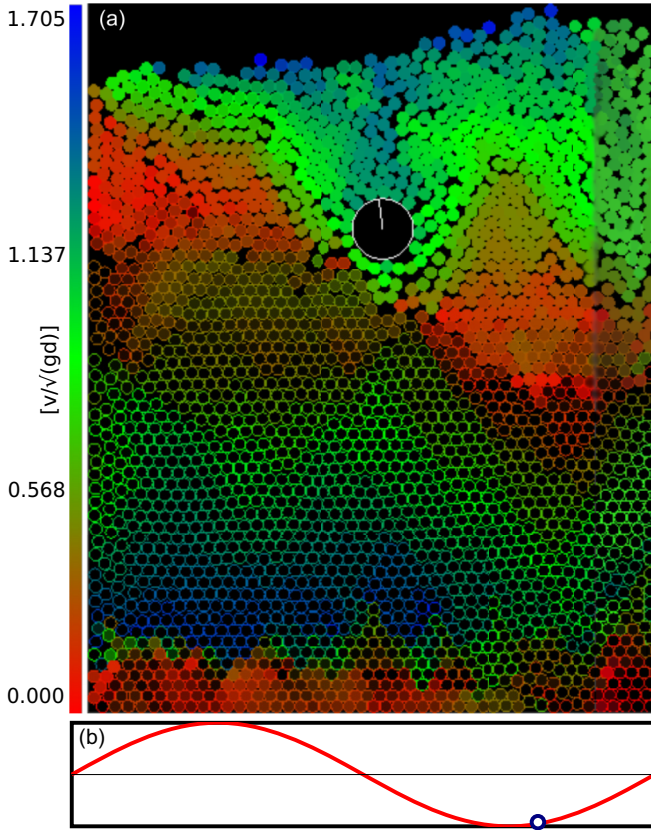


FIG. 1. (a) A typical snapshot of the system studied. Grains are represented by discs: hollow discs (\circ) are moving downward while filled ones (\bullet) are moving upward (against gravity). Color level shown at left side indicates the magnitude of the speed: red indicates no movement while blue indicates the maximum value for the speed. It is worth noting the inertia of the intruder accelerating the grains above him (bluish grains). It is also possible to observe the transition between the grains rising and falling in the reddish region around the intruder, a characteristic responsible for the granular ratchet effect. While the intruder easily displaces the grains on the way up, he is unable to move the grains that descend due to the steric exclusion. (b) Sinusoidal displacement imposed to the substrate. This snapshot was taken after the minimum of the oscillation of the substrate, marked as a blue dot in this plot.

the periodic boundary condition case, the resonance plays a major role in the intruder ascent.

In Sec. II, we present the simulation model and the resonance. In Sec. III, we define the normalized ascent rate and study it in the framework of the large deviation theory. In Sec. IV, we present our final conclusions.

II. MODEL

We perform discrete element method (DEM) simulations in two dimensions using molecular dynamics code [23] considering dry granular simulations, and a geometry design inspired in experimental setup. A hard core potential is used in a discrete element code with a third-order [23] gear-predictor-correction scheme. A sample in Fig. 1 shows us that most of the grains below the intruder are falling, while most grains above the intruder are rising. This snapshot reveals the gran-

ular ratchet mechanism: the grains below the intruder act as a solid while the grains above are displaced by the intruder's inertia and moving to below it. Two sets of simulations are analyzed with different boundary conditions: a usual geometry with frictional walls, and another with periodic boundary conditions (pbc) in the horizontal direction. We opted for this geometry to avoid steric exclusion induced by walls that enhances the granular ratchet effect. In this way, we expect to identify the specific contribution of convection to the segregation mechanism. Although other studies considered frictionless walls to avoid convection [24,25], we study BNE considering pbc.

The choice of studying the cases of pbc and frictional walls (fw) is a natural one when trying to determine the role of the walls in the ascent of the granular intruder. It is clear that the presence of frictional walls is responsible for the rise of convection currents formed due to the frictional contact of the moving grains and the wall. In Fig. 1 (fw), the asymmetry of the motion already shows the effect of those currents. Using pbc eliminates any symmetry breaking effect in this regard. The intruder ascent can no longer be explained by convection driving: it has to have a different cause. We shall see that it occurs, very slowly, in a limited range of frequencies, which suggest that the rising is akin to some resonant effect emerging from the complex behavior of the grains.

A. Setup

The sample preparation consists of depositing 2500 grains on a 37.5 grain-diameter wide substrate. The intruder is placed in such way that, after the deposition is finished, it remains stationed a few grains above the substrate. The intruder is a disk with radius 2.5 times as large as the average radius of other grains, with the same material density and stiffness though. The dynamics of the discs (grains) is implemented considering the modified Cundall-Strack rheological model [26] and the contact forces are modeled by two terms: an elastic component, represented by normal and tangential springs, and a viscous term, equivalent to a damper. We neglected damping in the tangential direction and thus Coulomb's friction dissipates energy along it. That is a quite fair approach as grains are subjected to an intense agitation and most of the contacts are very short lived.

Regarding the microscopic parameters, they were chosen with the objective of obtaining the best performance of the code. The base definitions of the standard units can be found in Atman *et al.* [27]; basically, we considered the average grain's diameter as a unit of length, the grain average mass is taken as unit of mass, and the gravity is a unit of acceleration. All the remaining units are derived from them. That means that the normal and tangential spring stiffness are equal to $k_n = 1000$, $k_t = 750$, respectively, and both kinetic and static friction coefficients are equal to $\mu = 0.5$. The damping coefficient is chosen so that the contact between the smallest grains of the system is supercritical.

We performed a set of simulations applying an external vibration that imposes a sinusoidal vertical displacement to the substrate with frequency ω and amplitude A . Depending on the parameter values, this forced sinusoidal field induces a solidlike to fluidlike transition at each oscillation [15]. These

regimes are associated with the nature of the interactions between the intruder and the surrounding media. As we previously noted, in Ref. [15] it is argued that for $\Gamma > 1$, and when the system is being pushed upwards, the granular medium behaves like a fluid and the intruder pushes the grains around it, due to its larger inertia. When the oscillation reaches its minimum, the grains below the intruder act like a solid due to the force chains formed from the substrate and the intruder becomes trapped. For pbc, we never observed the intruder rising for $\Gamma \leq 1$, while it is easily checked for the fw case. Another peculiar characteristic of the pbc case is the much longer time for the intruder to reach the surface, as can be seen in the horizontal axis of Figs. 2(b) and 2(c). Results were averaged over five samples.

B. Resonance

In analogy with the role of damping in traditional resonance analysis, the nonmonotonic behavior of the intruder vertical velocity distribution is a plain indication of resonant behavior in the system [28] since, for each value of Γ , there is a specific resonance frequency range where the maximum ascent rate occurs [please, see Figs. 2(d) and 2(e)]. This distinct behavior cannot be explained by the reverse buoyancy argument; note that Fig. 2(e) was built using the data from the system with pbc, so there is no wall-induced convection. The similarity with the forced damped harmonic oscillator problem can be evidenced as follows.

Hence, from those aforementioned results in the literature it can be concluded that granular ratcheting due to wall-induced convection [16] is the main mechanism acting on the BNE. On the other hand, when pbc are considered, the granular ratchet argument in itself fails to actually explain the intruder ascent rate behavior (see Fig. 3), which depends on ω given a fixed Γ . That dependency on ω is expected for a typical resonant system. The ascent rate is measured by considering the intruder vertical displacement after a certain elapsed time interval that is the same for all samples. The normalization was achieved by dividing the abscissa by the corresponding natural frequency ω_0 , adjusted by Eq. (2). Using that scaling, it is clear the system behaves like a forced damped harmonic oscillator, and thus resonant modes should appear.

To validate the approach of the system as a resonant oscillator and validate the analogy between the ascent rate and the sharpness curve as plotted in Fig. 3, we perform a fitting of the ascent rate curves in function of the frequency by means of the transmissibility function $G(\omega)$ that corresponds to the solution of the damped harmonic oscillator differential equation

$$\frac{d^2y}{dt^2} + 2\zeta\omega_0\frac{dy}{dt} + \omega_0^2y = \Gamma \sin(\omega t), \quad (1)$$

where ω_0 is the natural frequency of the system and m is the average mass of the grains, ζ is the damping ratio, a parameter of the fitting function. The solution to this equation can be written in several forms depending on the element over which is measured the response. Considering the resonant system in analogy to a RLC circuit, composed by a Resistor (R), an

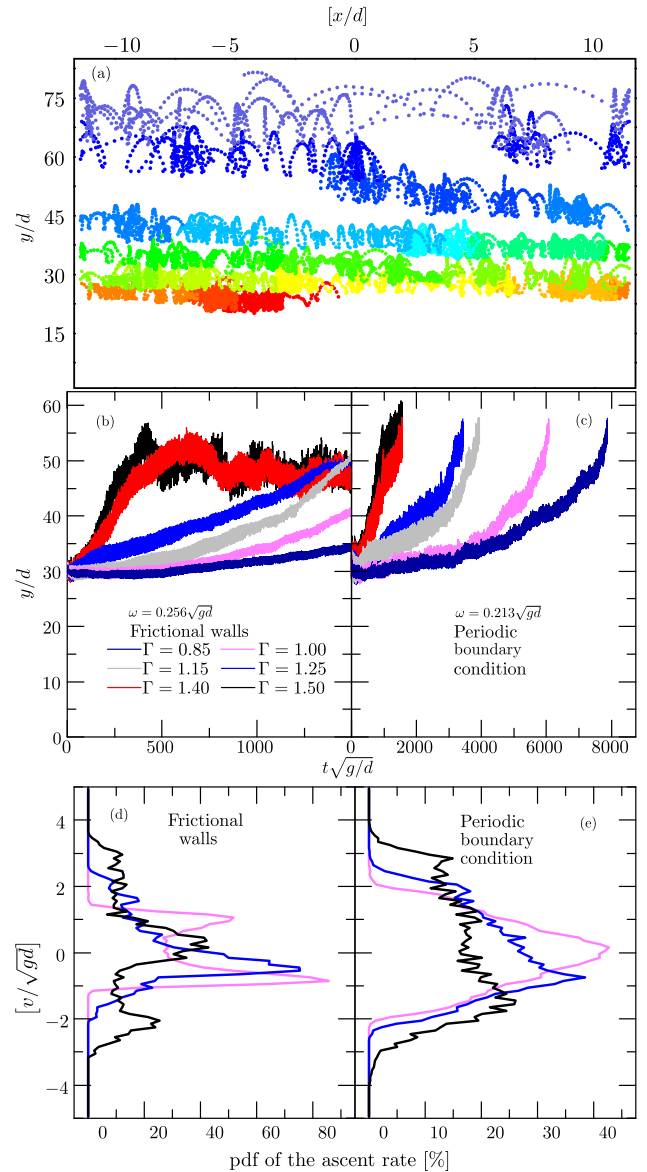


FIG. 2. (a) Sequential positions of the intruder (x, y) taken at constant time intervals (1000 molecular dynamics steps), for a system with periodic boundaries in the horizontal direction. $y = 0$ indicates the box floor and the unities are in unities of the mean grain diameter. The change in colors indicates the time elapsed in the simulation, the red corresponds to the beginning of the simulation and the blue to the end. As the color changes, it is possible to verify that the intruder crosses the periodic boundary several times. Middle panels: time series for intruder horizontal position at different Γ for system with (b) fw or (c) with pbc. In (b), simulations run until $2000\sqrt{d/g}$, while in (c) simulations run until the intruder rises beyond the highest grain. (d, e) Corresponding probability distribution functions (PDFs) of the intruder speed. Note the asymmetry features of PDFs. In the panels, d is the average grain diameter, t is the time, g is the gravity, v is the vertical intruder velocity, ω is the external frequency, and Γ is the normalized magnitude of the imposed acceleration. Legend presented in panel (b) applies to panels (b), (c), (d), and (e) equally.

Inductor (L), and a Capacitor (C), if we measure the transfer function over the resistive element, which represents the ascent

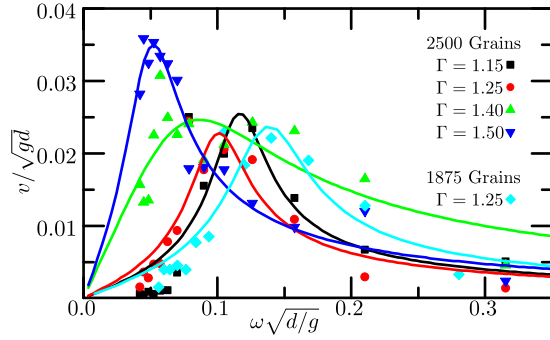


FIG. 3. Intruder ascent rate v curves for various normalized external accelerations Γ for the pbc case. $\Gamma = 1.15$ and 2500 grains is in \blacksquare , $\Gamma = 1.25$ and 2500 grains is in \bullet , $\Gamma = 1.40$ and 2500 grains is in \blacktriangle , $\Gamma = 1.50$ and 2500 grains is in \blacktriangledown , $\Gamma = 1.25$ and 1875 grains is in \blacklozenge , all with $37.5d$ wide.

rate of the intruder, the solution for the gain reads

$$G(\omega) = \frac{2\xi\omega_0\omega}{\sqrt{(2\xi\omega_0\omega)^2 + (\omega_0^2 - \omega^2)^2}}, \quad (2)$$

which we used to fit the data in Figs. 3 and 4. Note the bell shape of the fitting curves, analogous to the sharpness curve for the amplitude magnitude typical in traditional resonance analysis.

It is worth mentioning that Rivas *et al.* [29] studied several granular systems with walls and with pbc as well as concluding that convection only plays a significant role above ~ 33 rad/s for both systems. It is worth noting that we worked within a range of frequencies one order of magnitude smaller than that threshold; there is no significant convection contribution in the pbc, and we can disregard this source of transfer of moment to the intruder.

Bearing in mind that the intruder is initially placed near the bottom of the system, the periodic external force has the

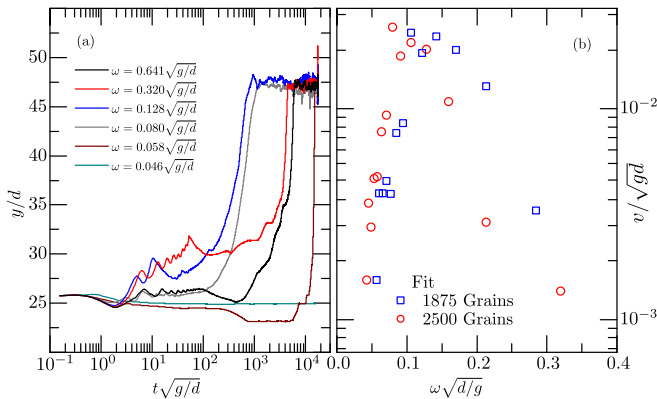


FIG. 4. Left: Intruder position in function of time for $\Gamma = 1.25$ for pbc and different imposed frequencies exhibiting a nonmonotonic behavior as the frequency increases. Right: Ascent rate curves for two different system sizes with pbc. 1875 grains in \square , 2500 grains in \circ . The normalization was made by dividing the abscissa corresponding to the larger system by the ratio of system sizes. These results were taken from a single sample.

effect of making the intruder vibrate vertically by small displacements [see the initial segments of the trajectory, in red, in Fig. 2(a)]. Consistently with that argument, we found that this shock-wave hits the intruder periodically at the very beginning of an upwards movement, accelerating it upwards to make a large jump, leading to the resonant behavior. After jumping to a higher position, the downwards movement is again blocked by the granular media, resulting in the ratchet effect. It can be expected that, as the distance between the intruder and the lower wall increases, the resonant frequency decreases since the shock wave velocity is approximately constant. However, the speed of the shock wave depends on the apparent density and, as it varies continuously due to the influx of external energy, the time interval between the jumps is not constant and too complex to estimate as well. To ensure this interpretation is correct, we decided to run simulations with another system size and compare resonant frequencies.

Figure 4(b) shows the resonance curve normalized for two different systems under pbc, with 1875 and 2500 grains, respectively. The linear dependence of the scaling factor with the system size is another hallmark of resonance phenomena. Figure 4(a) shows the intruder individual trajectories for each frequency tested. Note the characteristic emblematic behavior of the frequency 0.058 curve: the intruder remains almost motionless for the first 10 000 time units (even experiencing a slight dip) and suddenly rises to the surface. This sudden rise, characterized by large leaps, is a further evidence that resonance is acting on the intruder displacement.

III. LARGE DEVIATION THEORY

In Ref. [30] it was demonstrated experimentally that the motion of a self-propelled large particle, driven only by the asymmetry of its shape, could be shown to exhibit fluctuation properties that were a symmetry property of a large deviation function of an appropriate quantity related to its horizontal motion. The BNE also exhibits the same characteristic ratcheted motion, albeit in the vertical direction. It is important to check whether the same hidden fluctuations might be behind the intruder's motion.

Basically, we are interested in quantifying the fluctuations of the ascent rate distribution of the intruder. For this, we measure the normalized W_τ [30]

$$W_\tau(t) = \frac{1}{\tau} \int_t^{t+\tau} \frac{v(t')}{\langle v \rangle} dt', \quad (3)$$

where $v(t)$ is the intruder vertical velocity at time t and $\langle \cdot \rangle$ denotes the average over $[0, t + \tau]$. Next, we calculated $P(W_\tau)$, the density probability function of W_τ , and obtained the rate function (RF) at the limit

$$\text{RF}(W_\tau) = - \lim_{\tau \rightarrow \infty} \frac{1}{\tau} \ln P(W_\tau). \quad (4)$$

Taking into account that W_τ is analogous to the entropy production rate [30–32]¹, the linear response theory of

¹The entropy described here is the granular macroscopic entropy, which does not take into account the microscopic thermal entropy produced by the heat generating granular inelasticity.

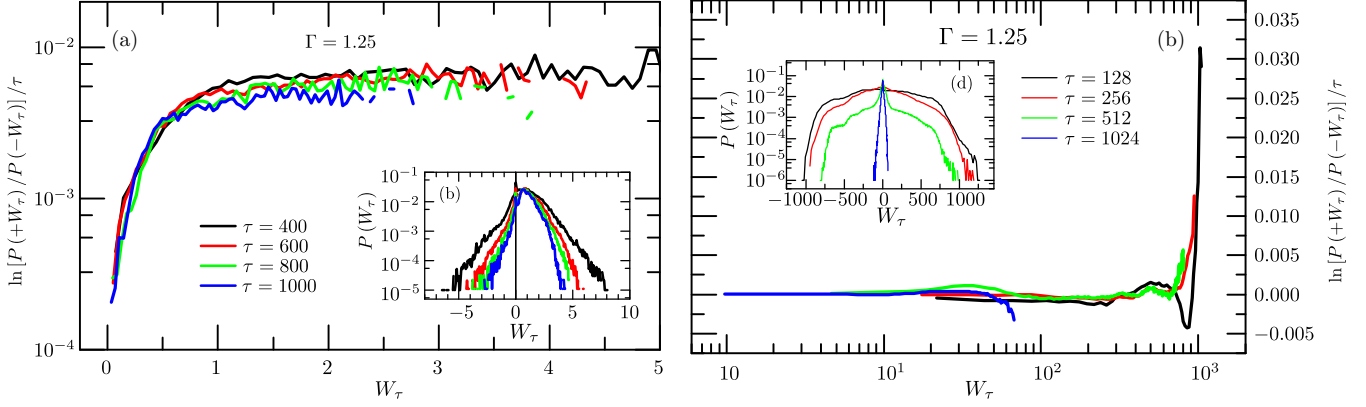


FIG. 5. Inset: $P(W_\tau)$ for $\Gamma = 1.25$ and several values of τ as shown in the legends, for both systems: with frictional walls at left and pbc at right. Main panels: Collapse of the RF function calculated for $\Gamma = 1.25$, and several values of τ . Data collapse was performed by dividing the ratio between upward and downward probabilities by the integration time τ . For the range of integration times considered, a remarkable collapse is observed. The frictional walls' case is shown at left and pbc at right panel. Observe that distributions for pbc are much more symmetric than those for fw, which lean strongly to the positive side.

fluctuation ratios (FR) predicts that $RF(W_\tau) - RF(W_{-\tau}) \sim W_\tau$. Thus, we measured that quantity under different BNE regimes and verified that the FR is valid for distinct time windows τ and different boundary regimes (pbc and with friction walls). In Fig. 5, we showed the ratio $1/\tau \ln P(W_\tau)/P(-W_\tau)$. The curves' collapse is noticeable for the range of integration times considered. As expected, we did not get a collapse for shorter integration times since the oscillatory feature of the external load dominated the dynamics for short times. Only for long integration times, when the BNE regime can be observed, did a good collapse occur.

The difference between the RF curves for systems with pbc and the walls' boundaries is striking, as shown in Fig. 5. When there are walls confining the system, we observe a strong asymmetry between downward and upward velocities, leading to high values of the RF, as shown in Fig. 5(c). On the other hand, when pbc was considered, the RF vanished for most W_τ values only showing significantly nonzero values for very large W_τ values. This observation concurs with the point that the convection induced by the walls is the main mechanism acting in the ascending of the intruder, when walls are present. For the pbc case, the RF shows that only for high values of

W_τ is an asymmetry observed in the upward and downward velocities, which is compatible with the fact that the larger jumps occur only when resonance takes place.

IV. CONCLUSION

In conclusion, we reported a survey on the Brazil Nut Effect considering systems with either frictional walls or periodic boundary conditions that put in evidence the leading role played by the resonance on the ascent rate of the intruder for the periodic boundary case. We reinforce our assertion by measuring the rate function for each distinct boundary case, and interpreting the difference observed in the results as a consequence of the different roles exerted by the walls and the resonance. As suggested by Kumar *et al.* [30], the phase-space contraction associated with the origin of the collapse in Fig. 5(b) only manifests itself for large values of W_τ . Our results significantly change the understanding of the BNE phenomenon and we expect that it will motivate experiments about this alternative approach for the problem. In a future

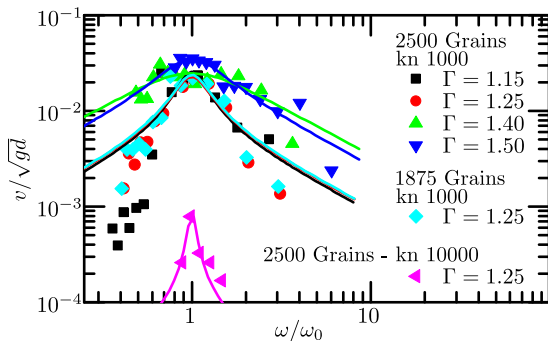


FIG. 6. Collapse of the measured values. The data points are collapsed for all simulations with pbc. The fit can cover the ascent rate for different parameters, like stiffness k_n , normalized acceleration Γ , and the column above the intruder h .

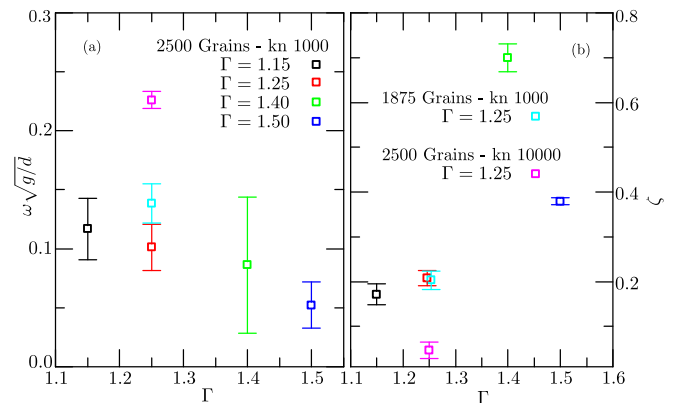


FIG. 7. Fit of the parameters using Eq. (2). In (a), the fitted natural frequency ω_0 shows little dependence with Γ . In (b), the dissipation parameter shows agreement within the error bars to a constant value.

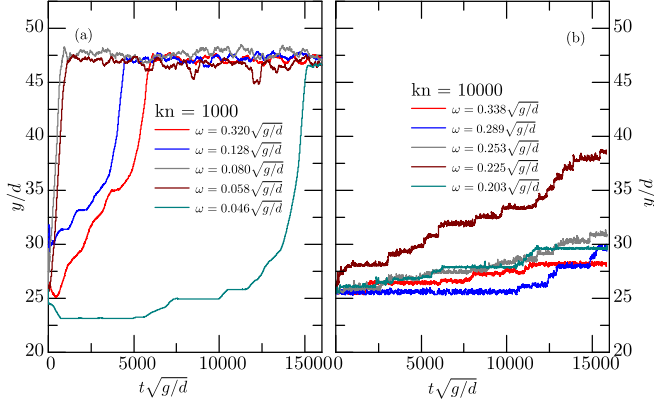


FIG. 8. Temporal profile, according to stiffness. Rising trajectories for the intruder. In (a), for lower hardness ($k_n = 1000$), we observe that the intruder can rise suddenly and fast. In (b), for a much higher hardness ($k_n = 10000$), the intruder only rises for a limited range of frequencies, and it clearly jumps each layer after some waiting time, with the possible exception of the case for the fastest rising rate ($\omega = 0.225\sqrt{g/d}$) where the waiting time is minimal.

work we plan the present large deviation analysis to quantify the contribution of each mechanism, especially resorting to an experimental setup.

ACKNOWLEDGMENTS

The authors would like to acknowledge the discussions with P. Claudin with relation to the idea of the resonance as a mechanism for the BNE. G.H.B.M. thanks CEFET-MG, CNPq, FAPEMIG, and CAPES Grant No. 88881.187077/2018-01 and especially P. Claudin. W.A.M.M. thanks CNPq and Faperj for financial support. A.P.F.A. and S.M.D.Q. thank CNPq Grants No. 301717/2019-2 and No. 308792/2018-1, respectively.

APPENDIX

We measured the ascent rate of an intruder inside a granular media to explain the resonance effect on the BNE in two dimensions with frictional walls (fw), frictionless walls (flw), and periodic boundary conditions (pbc). This Appendix contains some extra information about the fitting function used to describe the resonance effect and some other parameters, such as stiffness constants and different intruder densities.

1. Fitting function for resonance

We proposed in our study that, in the absence of confining walls, the BNE effect can be best explained by means of a resonance phenomenon. To quantify it, we collapsed the data with the function defined in Eq. (2), and normalized the values of the abscissa accordingly, where ω_0 is the bare natural frequency for a damped harmonic oscillator and ζ is the damping ratio, acting as a free fitting parameter.

The chosen function behaves as a linear band-pass filter, meaning that frequencies much lower and much higher than ω_0 are damped to zero values on its response, while near ω_0 the response is near to its peak. The transfer function

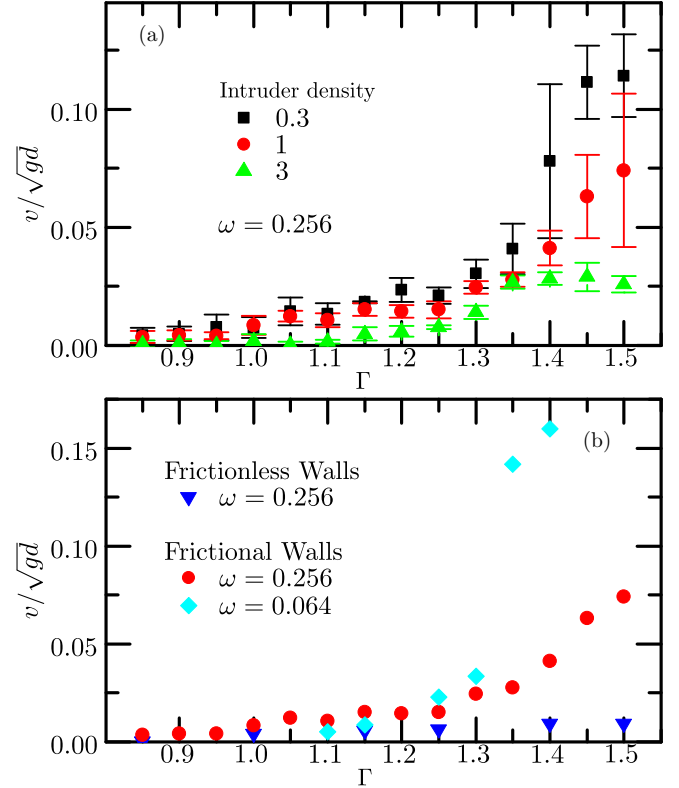


FIG. 9. In (a) the simulation was set to fw, width of $37.5d$, shaken frequency of $0.256\sqrt{g/d}$, 2500 grains, and we varied the intruder density, compared to the medium. In (b), a comparison between fw and flw and a change in frequency.

corresponds to the response on velocity, which also fits the dimension of the measured ascent rate.

To make the quantities dimensionless, we may use a set of variables such as the mass of the intruder m , the diameter of the grains d , and the gravity acceleration g . The normalization factor, based on the natural oscillation frequency ω_0 , is dependent on the height of the granular column h and on the square root of the stiffness of the material $\sqrt{k_n}$.

The fitting function was chosen to represent a damped harmonic oscillator near its resonance [Eq. (2)]. Although the BNE model is far from being a simple harmonic oscillator, there is a qualitative concordance of the simulation results with those of the simple resonant model.

In Fig. 6, we depict the fitting, done according to Eq. (2), where we can see that the qualitative behavior of the BNE near the peak value for the ascent rate is well described by the resonance model. Even for very hard particles $k_n = 10000$, the model describes reasonably well the frequency dependence for the ascent rate.

We also fitted the parameters ω_0 and ζ , as can be seen in Fig. 7. For the range of Γ studied, the values of the dissipation factor ζ are compatible within the error bars. For the natural frequency ω_0 , the fittings suggest that the values are almost constant for a broad range of values of Γ .

Beyond testing the resonance hypothesis, we can turn up the stiffness constant and observe its effect on the ascent rate. This is done in Fig. 7.

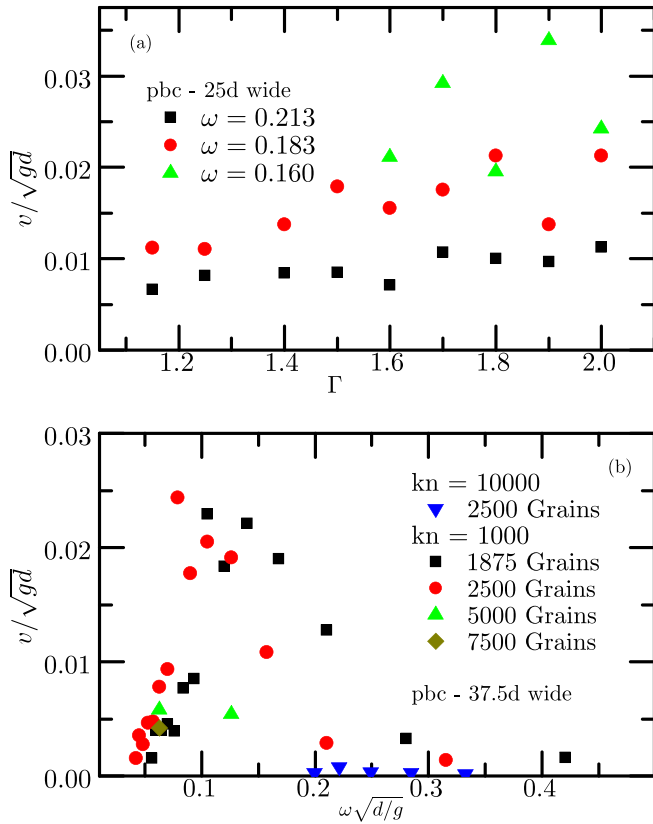


FIG. 10. In (a) 25d wide in pbc. Increase Γ leads to increase ascent rate. In (b) 37.5 wide in pbc.

2. Harder grains in simulations under pbc

To check the results in the resonance region, we ran a series of simulations for harder particles (intruder and grains),

$k_n \sim 10\,000$. For harder particles, their collision duration time is reduced ($t_{col} \propto k_n^{-1/2}$ for harmoniclike interactions).

For the hard-particle case, we verified the resonance effect becomes sharper, which can be seen clearly for the fit we obtain [see Fig. 3(b)]. Concerning the individual trajectories, jumps become much more rare and, even on the top of the resonance frequency range, one can observe the BNE rises by a granular layer at a time [see Fig. 8(b)].

As seen above, only at a very specific frequency ($\omega = 0.225\sqrt{g/d}$ in Fig. 8) the height increments accumulate quickly, suggesting that at that characteristic frequency a collective behavior emerges due to resonance.

Those jumps are indeed rare events along the overall movement of the intruder, therefore, we would like to analyze them from the point of view of the RF [33,34]. This approach was successfully applied to an anisotropic intruder, confined by a granular material, by Ramaswamy *et al.* [30]. Here, we decided to apply this approach to obtain the RF for the BNE regime for both with pbc and walls. It is worth mentioning that, unlike in Ref. [30], our intruder is symmetrical (gravity breaks the symmetry) and oscillations are imposed along the vertical displacement direction of the intruder.

The problem with fw has a significant difference, if compared with pbc. The ascent rate is at least one order of magnitude larger, and this property is seen in the large deviation response. Comparing the difference of density between the intruder and medium, we expect that the lighter intruder arise more quickly than heavier ones, and fw contribute more than fw. Figure 9 shows us that increasing Γ usually increases the ascent rate.

In pbc, the greater the granular column, the narrower the width band. The same applies to the stiffness increase. The left panel in Fig. 10 has 25d width in three different frequencies, the right panel has 37.5d width in ω , with different granular columns.

- [1] J. Duran, *Sands, Powders, and Grains: An Introduction to the Physics of Granular Materials*, Partially Ordered Systems (Springer, New York, 1999).
- [2] H. M. Jaeger, S. R. Nagel, and R. P. Behringer, *Rev. Mod. Phys.* **68**, 1259 (1996).
- [3] A. Mehta, *Granular Physics* (Cambridge University Press, Cambridge, England, 2007).
- [4] H. Herrmann, J. Hovi, and S. Luding, *Physics of Dry Granular Media*, Nato Science Series E (Springer, Amsterdam, 2013).
- [5] B. Andreotti, Y. Forterre, and O. Pouliquen, *Granular Media: Between Fluid and Solid* (Cambridge University Press, Cambridge, England, 2013).
- [6] S. F. Edwards and R. B. S. Oakeshott, *Physica A* **157**, 1080 (1989).
- [7] P. G. de Gennes, *Rev. Mod. Phys.* **71**, S374 (1999).
- [8] H. Hinrichsen and D. Wolf, *The Physics of Granular Media* (Wiley, New York, 2006).
- [9] N. Brilliantov and T. Pöschel, *Kinetic Theory of Granular Gases*, Oxford Graduate Texts (Oxford University Press, Oxford, 2010).
- [10] D. C. Hong, P. V. Quinn, and S. Luding, *Phys. Rev. Lett.* **86**, 3423 (2001).
- [11] I. S. Aranson and L. S. Tsimring, *Rev. Mod. Phys.* **78**, 641 (2006).
- [12] J. M. N. T. Gray and C. Ancey, *J. Fluid Mech.* **779**, 622 (2015).
- [13] A. Tripathi and D. V. Khakhar, *J. Fluid Mech.* **717**, 643 (2013).
- [14] Y. Duan, P. B. Umbanhowar, J. M. Ottino, and R. M. Lueptow, *Phys. Rev. Fluids* **5**, 044301 (2020).
- [15] A. Rosato, K. J. Strandburg, F. Prinz, and R. H. Swendsen, *Phys. Rev. Lett.* **58**, 1038 (1987).
- [16] T. Pöschel and H. J. Herrmann, *Europhys. Lett.* **29**, 123 (1995).
- [17] M. E. Mobius, B. E. Lauderdale, S. R. Nagel, and H. M. Jaeger, *Nature (London)* **414**, 270 (2001).
- [18] M. Alam, L. Trujillo, and H. J. Herrmann, *J. Stat. Phys.* **124**, 587 (2006).
- [19] A. Sarracino, D. Villamaina, G. Gradenigo, and A. Puglisi, *Europhys. Lett.* **92**, 34001 (2010).
- [20] J. B. Knight, H. M. Jaeger, and S. R. Nagel, *Phys. Rev. Lett.* **70**, 3728 (1993).

- [21] S. H. Chou, C. C. Liao, and S. S. Hsiau, *Phys. Fluids* **23**, 083301 (2011).
- [22] J. A. F. Balista and C. Saloma, *Granular Matter* **20**, 47 (2018).
- [23] M. Allen and D. Tildesley, *Computer Simulation of Liquids* (Clarendon, Oxford, 1989).
- [24] J. A. C. Gallas, H. J. Herrmann, T. Pöschel, and S. Sokołowski, *J. Stat. Phys.* **82**, 443 (1996).
- [25] H. Herrmann and S. Luding, *Continuum Mech. Thermodyn.* **10**, 189 (1998).
- [26] P. A. Cundall, Strack, and O. D. L. Strack, *Geotechnique* **29**, 47 (1979).
- [27] A. P. F. Atman, P. Claudin, and G. Combe, *Comput. Phys. Commun.* **180**, 612 (2009).
- [28] M. Trulsson, M. Bouzid, P. Claudin, and B. Andreotti, *Europhys. Lett.* **103**, 38002 (2013).
- [29] N. Rivas, A. R. Thornton, S. Luding, and D. van der Meer, *Phys. Rev. E* **91**, 042202 (2015).
- [30] N. Kumar, S. Ramaswamy, and A. K. Sood, *Phys. Rev. Lett.* **106**, 118001 (2011).
- [31] G. Gallavotti and E. G. D. Cohen, *J. Stat. Phys.* **80**, 931 (1995).
- [32] G. Gallavotti, *Phys. Rev. Lett.* **77**, 4334 (1996).
- [33] H. Touchette, *Phys. Rep.* **478**, 1 (2009).
- [34] A. Vulpiani, F. Cecconi, M. Cencini, A. Puglisi, and D. Vergni, *Large Deviations in Physics* (Springer, Berlin, 2014).